CrossMark

ORIGINAL ARTICLE

He–Ne laser induced changes to CN-85 polymer track detector

M.F. Zaki *

Experimental Nuclear Physics Department, Nuclear Research Center, Atomic Energy Authority, P.O. 13759 Abu Zaabal, Cairo, Egypt
Medical Physics Department, Faculty of Medicine, Jazan University, Saudi Arabia

Abstract   In this work, the induced changes in cellulose nitrate (CN-85) polymer track detector have been investigated. CN-85 samples were irradiated with He–Ne laser at different fluences. These investigations have been carried out using UV–Vis spectroscopy, photoluminescence (PL) spectroscopy and X-ray diffraction (XRD). In addition, the wetting property and surface free energy (SFE) of the irradiated samples have been studied by measuring the contact angle. The UV–Vis spectra showed that the absorption edge shifted towards longer wavelength region with increasing irradiation. This means that the optical band gap energy was decreased by increasing the laser beam doses. The correlation between the number of carbon clusters and the optical band gap energy is discussed. The PL spectra indicated a decrease in the integrated photoluminescence intensity of irradiated samples compared with the pristine one. XRD intensity showed a dominant amorphous with a partly crystalline phase. The surface wettability was evaluated by contact angle method (for water, dimethyl-formamide and glycerol), as well as, the surface free energy which was estimated using Owens–Wendt method. Furthermore, the surface roughness has been studied.

1. Introduction

Over the past decades, there has been considerable interest in the study and improvement of the physical properties of polymeric materials. Solid state nuclear track detectors (SSNTDs),

due to their excellent properties are used in many applications ranging from daily life to high technology (Hermsdorf, 2011; Vijay Kumar et al., 2011; Steckenreiter et al., 1997). SSNTDs are made from special polymers that are used as biological filters, sensors and dosimeters. Cellulose nitrate (CN-85) is one of the SSNTDs. Nowadays, the irradiations of polymer materials are widely used to improve the physical and chemical properties for appropriate and high technology applications (Ramola et al., 2009; Srivastava et al., 2002; El-Badry Basma et al., 2009; Rizk et al., 2008; Sharma et al., 2007; Radwan, 2009; Singh and Prasher, 2005). As a result of the passage radiation through materials, the radiation energy is absorbed by the materials through the occurrence

* Tel.: +20 1002718565; fax: +20 0173217540.
  E-mail address: moha1016@yahoo.com.
Peer review under responsibility of King Saud University.

of irreversible changes in the macromolecular structure of that material. These changes lead to bond breaking, main chain scission, creation of unsaturated bonds, intermolecular cross linking, radical composition, loss of volatile fragments etc., (Zhiyong et al., 2000; Phukan et al., 2003; Abdul-Kader et al., 2012; Marletta, 1990; Calcagno et al., 1992; Abel et al., 1995; Klaumiinzer et al., 1996; Bouffard et al., 1997). Previously, a comparison has been investigated on the effect of laser beam on the optical properties of CN-85 and CR-39 irradiated with alpha particles. This investigation mainly aimed to study the effect of electromagnetic radiation on the etching parameters and optical properties of the irradiated samples with charged particles (Zaki et al., 2014). To complement this study, the principle objective of the present work is to enhance the optical, photoluminescence and structure properties, as well as, the wettability and surface free energy through laser beam induced modifications to use this polymer in suitable medical and industrial applications.

2. Materials and methods

The CN-85 samples used in this study were cut from the commercially available sheet with thickness 100 μm. CN-85 have a density of 1.54 g/cm^3 manufactured by Eastman Kodak Company, Rochester, New York. The CN-85 samples were irradiated with He–Ne laser beam with energy 5 mW with different fluences up to 400 J/cm^2. All irradiations were performed with set up to keep the homogeneity of the laser beam on the sample surface. A square mask was used to define the laser beam incidence onto the sample surface, while a uniform fluence at the sample surface was obtained by using a beam homogenizer. The changes in the optical absorption induced by the laser beam and energy band gaps of the pristine and irradiated CN-85 polymers were measured using UV–Vis Spectrometer (Jasco, Model V-670) with a scan speed of 200 nm/min, in the range of 200–900 nm. To investigate the irradiation induced disorder, the PL spectra were recorded using the Spectrofluorophotometer (RF-1501 SHIMADZU, Ltd.) in the wavelength ranging from 200–900 nm at an excitation wavelength of 350 nm. CN-85 samples were characterized for their structural properties by using X-ray diffraction (Philips powder diffractometer, type PW 1390 goniometer) with a graphite monochromator crystal at room temperature. The wavelength of the X-ray was 1.542 Å and the diffraction pattern was recorded for a range of Bragg's angle (4–70°) with scanning speed of 2° per min. The wettability and surface free energy of the pristine and irradiated samples were determined by measuring the contact angle for three different liquids namely distilled water, dimethyl-formamide and glycerol. The used liquids were selected to cover the possible range from very disperse liquid (dimethyl-formamide) to a very polar liquid (water). For each liquid three drops were put on the sample surface using micro-syringe. Digitalized images of the liquid drops were captured and analyzed to determine the contact angle value. The surface free energy was estimated using Owens–Wendt method (Owens and Wendt, 1969). The Owens–Wendt method is the selected method to evaluate the surface free energy which is taking into account polar γ^p and dispersive γ^d components using at least two different liquids. The sum of the polar and dispersive components gives the total surface energy γ^t. The surface roughness R_a of the irradiated samples and the pristine one was measured using TR110 Surface Roughness Tester. Roughness R_a quantified by the vertical deviations of a real surface from its ideal form, was calculated by taking the average values of three measurements of each sample.

3. Results and discussion

3.1. UV–Visible analysis

Fig. 1 shows the optical absorbance on the pristine and irradiated CN-85 samples in the range 200–900 nm. It is clear that increases in the optical absorption for each irradiated samples were compared with the pristine sample. The increase in the optical absorption by increasing the laser dose might be attributed to the formation of new electronic levels in the forbidden band gap (Abdul-Kader et al., 2010). Moreover, it was observed that after irradiation the UV spectra were shifted from UV–Vis toward longer wavelengths, which might be due to the creation of conjugated bonds during the irradiation. The variation of absorbance difference $(A - A_o)$ as a function of irradiation dose is shown in Fig. 2. It is clear from the figure that the increase in the absorbance difference with the irradiation dose is linear within the given dose. This linear relationship opens the possibility to use the CN-85 polymer as a laser beam dosimeter, which is more effective and less time-consuming than the traditional ones. The optical band gap could be calculated from the absorption edge of the UV–Vis spectra of pristine and irradiated samples. Fig. 3 shows the relation between $(\alpha h v)^2$ and $(h v)$. The optical band gap was calculated by Tauc's expression from the extrapolation of the plot of $(\alpha h v)^2$ verses $(h v)$ on the $h v$ axes. The Tauc's formula (Abdul-Kader, 2013) is given by:

$$\alpha(h v) = B(h v - E_g)^2 / h v \tag{1}$$

α in such a situation is the absorption coefficient, whereas, $h v$ is the photon energy and E_g is the value of the optical energy gap. The dependence of E_g on the irradiation dose is shown in Fig. 4. The principle concept of calculation of the optical energy band gap was previously reported in Ref. (Zaki, 2008). It is clear that the optical band gap energy decreases by increasing the irradiation dose. There is 28% decrease in band gap value of irradiated sample with the highest dose. This might be attributed to the enrichment of carbon clusters formed and creation of conjugated system of bonds due to the partial growth of hydrogen gas (Abdul-Kader, 2013; Gupta et al., 2000).

It is known that the number of carbon atoms (N) in a cluster is correlated to the optical energy band gap, E_g. So, for more clarity, the number of carbon atoms per conjugated length N can be calculated by modified Tauc's equation (Abdul-Kader, 2009):

$$N = 2\pi\beta / E_g \tag{2}$$

where 2β gives the band structure energy of a pair of adjacent π sites and it is taken to be ~2.9 eV. It is clear from Fig. 4 that the number of carbon atoms N increases by increasing the laser dose. This increase leads to the escape of hydrogen, which is attributed to breakage of the C-H bond by energetic radiation. This increase in the number of carbon atoms N confirms the decrease in the optical band gap energy E_g which indicates
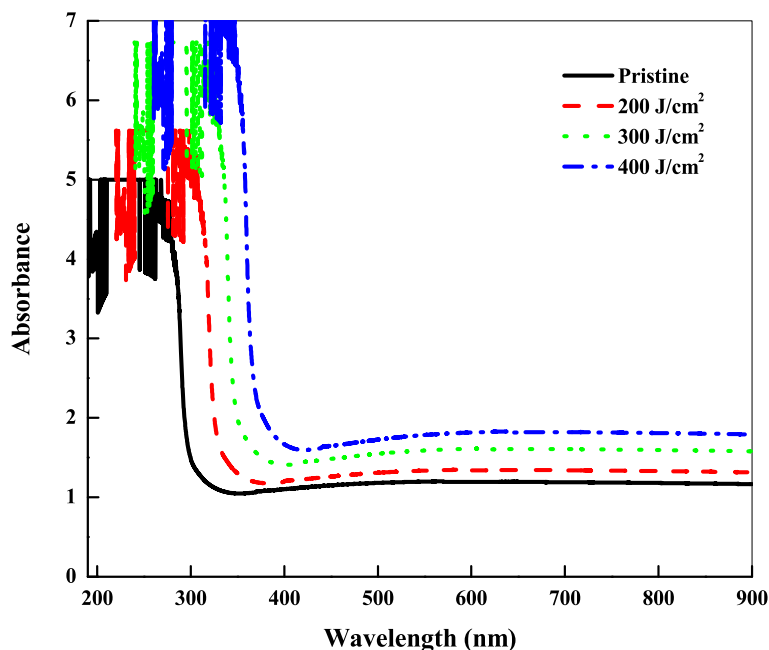
Figure 1 UV–Vis spectra of pristine and laser beam irradiated CN-85 polymer.
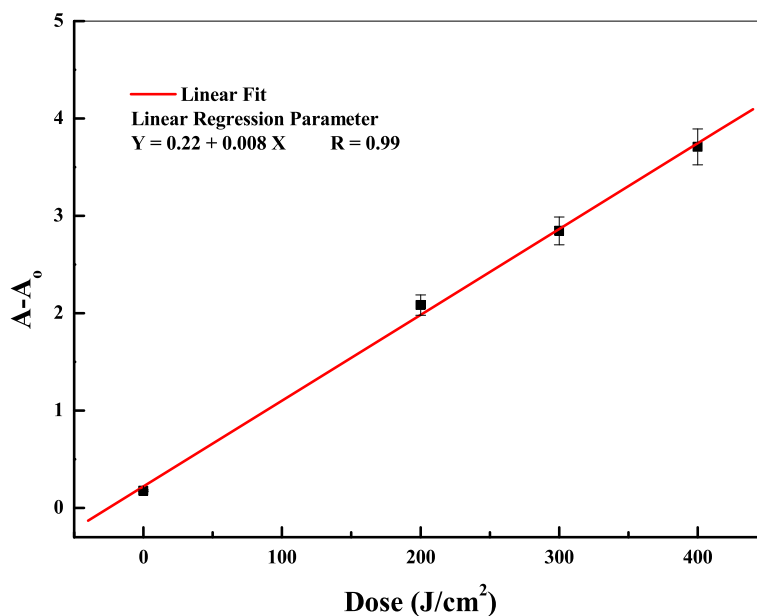

Figure 2 Plot of absorbance difference $(A - A_o)$ versus laser beam dose for CN-85 samples.

an increase to the electrical conductivity of polymers after irradiation with laser beam.

In order to bring to light the UV–Vis spectra, the thermal fluctuations in the band gap energy were estimated by the width of the band tail of the localized states in the band gap. This is called the Urbach's energy E_u. Urbach's energy was observed firstly by Urbach (1953) for silver halides as demonstrated by the following relation:

$$\alpha = \alpha_o exp(h\nu/E_u) \qquad (3)$$

where $h\nu$ is the photon energy, α_o is a constant; E_u is Urbach's energy which is equal to the inverse logarithmic slope of the

absorption coefficient and α is an absorption coefficient. Fig. 5a shows the dependence of $\ln(\alpha)$ on the photon energy $(h\nu)$ for pristine and laser irradiated CN-85 samples. The values of the Urbach's energy were calculated from the reciprocal of the slopes of the linear part in the lower photon energy region of the graph of $\ln(\alpha)$ as a function of photon energy $(h\nu)$. The changes in the Urbach's energy are shown in Fig. 5b. It is noticed that the Urbach's energy decreases by increasing the irradiation doses. The origin of E_u is a shift of the band gap energy. This is due to its dependence on the temperature as well as the self-energized electrons and holes interacting with the photons.
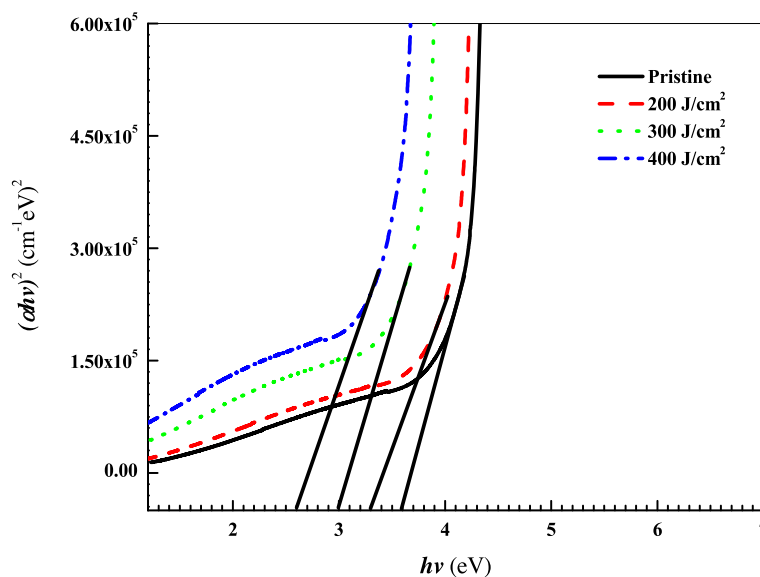
Figure 3   The dependence of $(\alpha h\nu)^2$ on photon energy ($h\nu$) of pristine and irradiated CN-85.
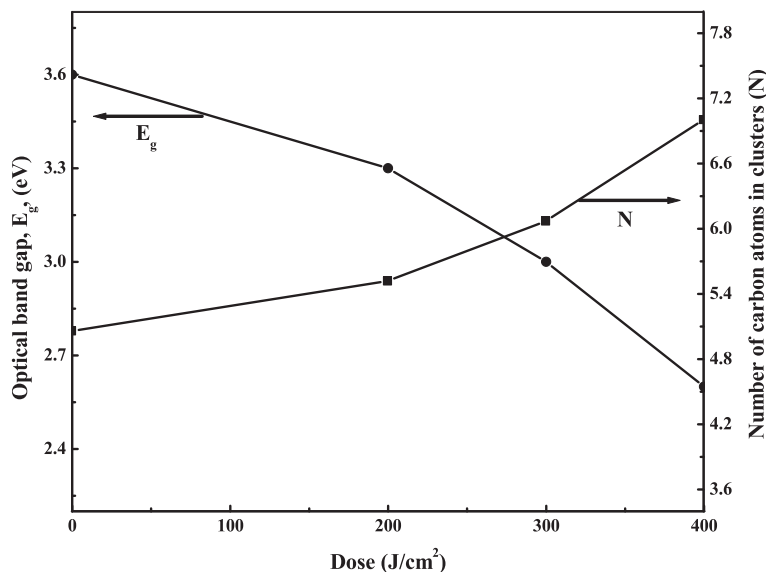

Figure 4   Optical energy gap and the number of carbon atoms in cluster of CN-85 as a function of laser dose.

3.2. Photoluminescence analysis

The PL spectra of pristine and irradiated CN-85 polymer are shown in Fig. 6. There is a remarkable significant decrease in the PL intensity with increasing the laser dose. This decrease in PL intensity is called hypo chromatic shift. This trend in the luminescence indicates the formation of new radiative recombination levels (Toth et al., 2006), which may be due to the increase of the energy deposited by the laser beam in the samples. Moreover, this decrease can be attributed to the changes in the electronic behavior, which is as a result of changes in the molecular structure of CN-85 polymer. The peak wavelength center (k_c) is observed at 720 nm for pristine sample and at 718, 716 and 714 nm for laser irradiated samples

with 200, 300 and 400 J/cm^2, respectively. It is clear from Fig. 6 that there is a small shift in the PL spectra by increasing the irradiation dose. This shift is called the bato chromatic effect. Furthermore, Fig 6 shows a difference between the positions of the band maxima of absorption and fluorescence of the same electronic transition. This difference ($h\nu_{ex} - h\nu_{em}$) is known as Stokes shift, and it is illustrated in Fig. 6. Stokes shift is essential to the sensitivity of fluorescence techniques because it allows for the emission of photons which are detected at low background, and which are isolated from excitation photons. Therefore, the Stokes shift is an important property to separate between the strong excitation light and weak emitted fluorescence by using suitable optics in the practical applications of fluorescence.
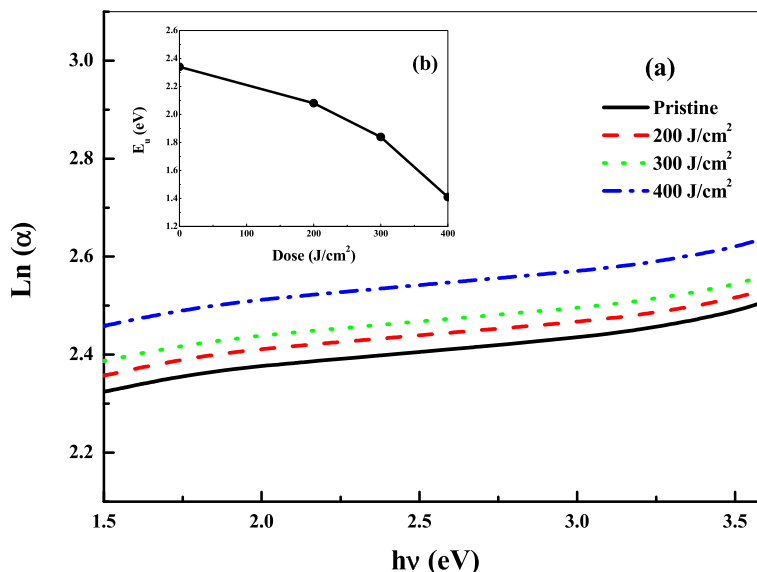
Figure 5 Dependence of natural logarithm of (α) on photon energy (a) and Urbach's energy E_u (b) of pristine and laser beam irradiated CN-85 polymer.
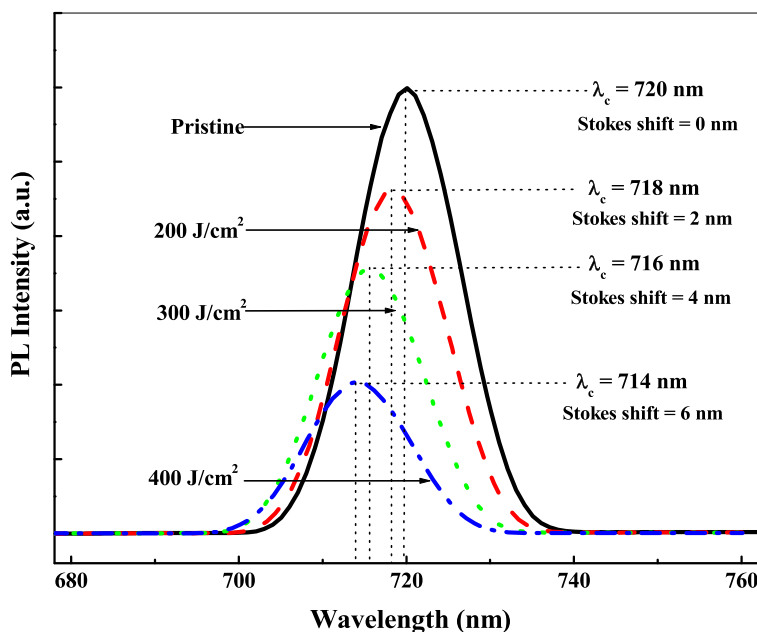

Figure 6 Photoluminescence emission spectra of pristine and laser beam irradiated CN-85 samples, the excitation wavelength is 350 nm.

3.3. X-ray diffraction analysis

It is known that most polymers are not entirely crystalline, because the chains or parts of chains have no order to the arrangement of their chains. So, a crystalline polymer has two phases, the crystalline portion and the amorphous portion. The existence of amorphous portion leads to the appearance of characteristic amorphous halos in the diffraction pattern. The XRD intensity of the pristine and irradiated samples is shown in Fig. 7. It is clear from the figure that the patterns of the samples are characterized by halos in the range of 12–25°. This indicates a dominant disordered atomic structure and therefore destruction of crystalline structure of the samples

(Radwan 2001). This might be attributed to the increase in the irradiation dose which could lead to cross linking, therefore bringing about reduction in the crystalline structure which suggested convergence of the polymer toward a more disordered system (Lounis-Mokrani et al., 2003). Any significant change appears in the peak intensity after irradiation leads to changes in the structure of the materials. As shown in Table 1, a gradual decrease in the integral intensity occurs with increasing the laser dose. This decrease can be explained by the decrease in the amount of crystalline phase in the irradiated samples, and consequently, destruction in the crystalline structure. This can be explained by the formation of new bonds between the neighboring chains, which may be attributed to
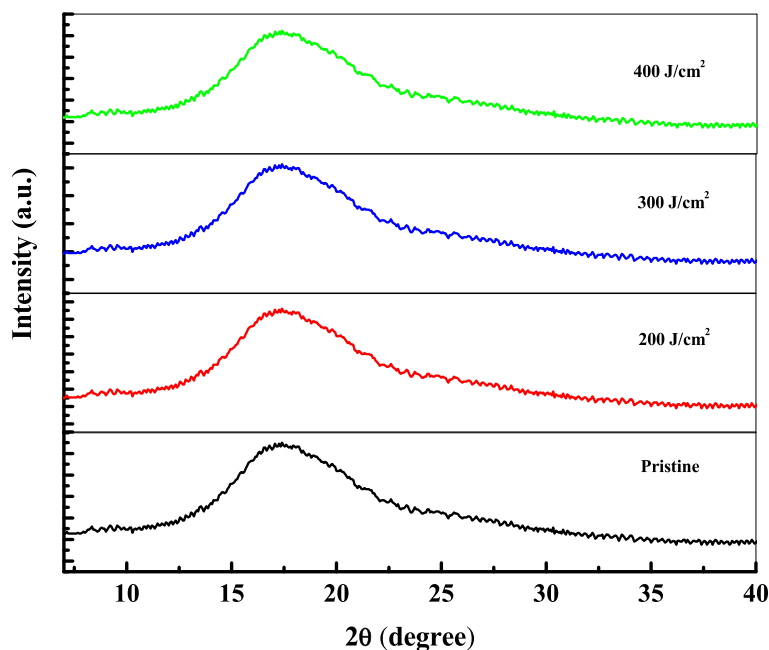
Figure 7 X-ray diffraction patterns of the pristine and laser beam irradiated CN-85 polymer.

Table 1 XRD parameters of laser irradiated CN-85 polymer track detector.

Laser dose (J/cm²)	2θ (deg.)	Integral intensity (a.u.)	FWHM (b)	L (Å)	r (Å)	d (Å)	ε	σ	g%
0	17.4	768	7.6	12.17	3.22	2.57	1.81	0.0067	24.26
200	17.8	709	8.3	11.18	3.15	2.52	1.97	0.0080	25.86
300	17.1	654	9.9	9.34	3.27	2.62	2.36	0.0114	32.16
400	16.8	573	10.4	8.86	3.33	2.66	2.48	0.0122	34.46

the change in the regularity of the arrangement of the crystallites into disorders as a result the cross linking of the molecular chains. In addition, an increase in the full width at half maximum from the diffraction pattern was observed, which indicates the decrease in the crystallinity of the irradiated polymers. To obtain the qualitative calculations of the improvement in the irradiated polymers, area under the diffraction peaks was estimated using the best fitting of the data as illustrated in Table 1. It is noticed from the table that the area decreases with increasing laser dose. This decrease leads to a decrease in the crystallinity and disorderness in the polymer structure. Moreover, the structure parameters such as, the crystalline size (L), interchain distance (r), interplanar distance (d) have been estimated using the relations:

$$L = \lambda/b\cos\theta \tag{4}$$

$$r = 5\lambda/8\sin\theta \tag{5}$$

$$d = \lambda/2\sin\theta \tag{6}$$

Furthermore, the micro-strain (ε), dislocation density (σ) and distortion parameters (g) were calculated as follows:

$$\varepsilon = b\cos\theta/4 \tag{7}$$

$$\sigma = 1/L^2 \tag{8}$$

$$g = b/\tan\theta \tag{9}$$

here k = 1.542 Å is the wavelength, b is the FWHM of the diffraction peak, θ is the Bragg angle and k is the Scherrer constant and it is equal to unity. It can be observed from Table 1 that both the crystal size and integral intensity decreases with increasing laser dose. In addition, no significant changes were observed in the interchain and interplanar distances, because the change of angle of the peak intensity is slight after laser irradiation. Furthermore, an increase was observed with increase in the laser dose for the micro strain, dislocation density and distortion parameters. This increase may be attributed to the increase in the disordering of the irradiated samples.

3.4. Surface wettability and roughness

The dependence of liquids' contact angle on the laser irradiation doses is shown in Fig. 8. It is clear that the contact angle of pristine is higher compared with the irradiated samples. In case of pristine sample, the contact angle decreases from 89, 82 and 38 for water, glycerol and dimethyl-formamide, respectively to 62, 61 and 20 at the highest dose of laser beam. Generally, the contact angle values decrease with increasing the laser doses (Abdul-Kader 2013), which means that the wetting property of the irradiated samples is modified
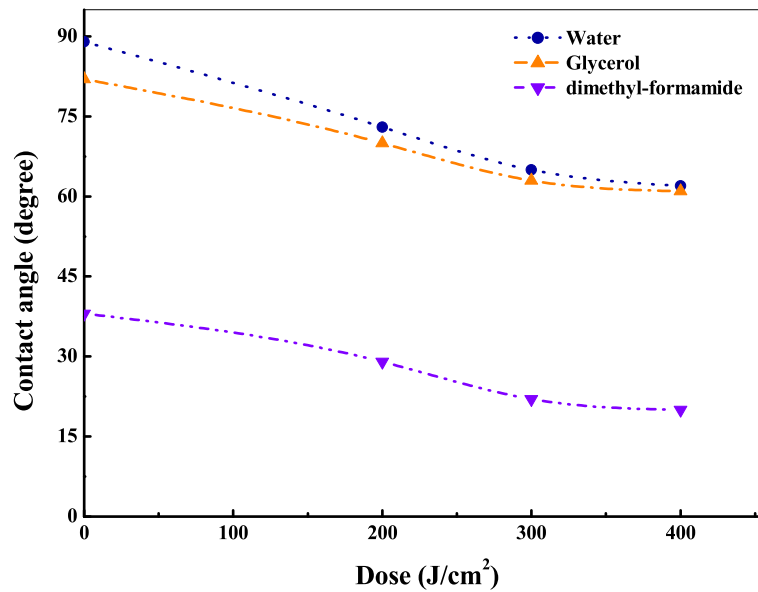
Figure 8   Variation of liquids' contact angle on CN-85 surface as a function of laser beam dose.

(Abdul-Kader 2009). It is well known that the micro-pores formed by the surface roughness have an effect on the wetting property of the samples. So, the surface roughness is measured for pristine and irradiated samples. It is found that the surface roughness R_a has fluctuated values of, 0.8, 0.6, 0.7 and 0.4 μm for the irradiation doses 0, 200, 300 and 400 J/cm^2, respectively. This means that the surface roughness is independent on the irradiation dose. Therefore, there is no linear relevance between the surface roughness and the irradiation dose. This means that the decreases in the contact angle of used liquids cannot be explained by the surface roughness, but may be due to the formation of hydrophilic groups which is formed by the creation of free radicals on the surface of polymer (Ali et al., 2013; Turos et al., 2006).

3.5. Surface free energy (SFE)

The variation of surface free energy as a function of laser doses is shown in Fig. 9. It was found that the SFE is increased by increasing laser dose from 34 mJ/m^2 for pristine sample to 41 mJ/m^2 for irradiated sample with the highest dose. In addition, the polar component is increased with increasing the irradiation doses. This increase is attributed to the production of polar groups on the sample surface. However, the increase in the laser dose, as found, decreased the dispersive component from 29 mJ/m^2 for pristine sample to 18 mJ/m^2 for irradiated sample with the highest dose. This decrease may be attributed to the formation of oxidation product on the irradiated surface samples (Ali et al., 2013).
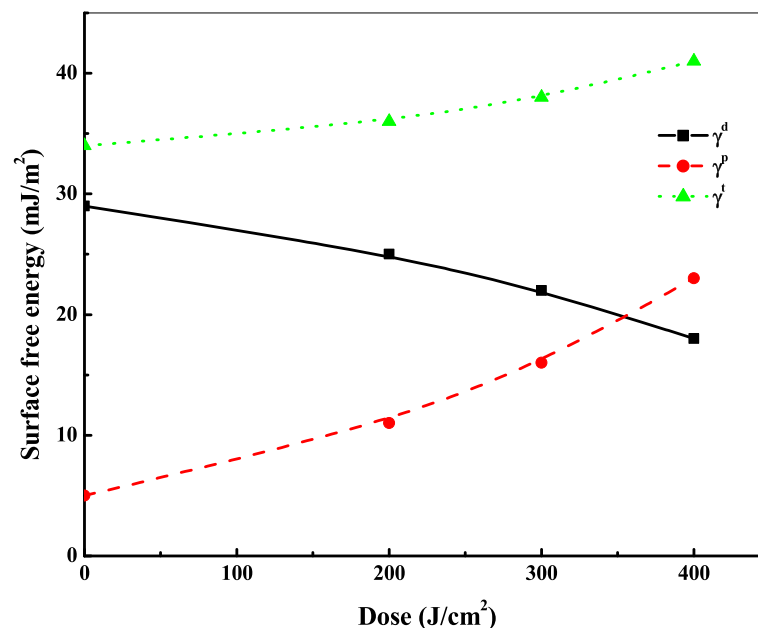

Figure 9   Surface free energy, dispersion and polar components of CN-85 as a function of laser dose.

4. Conclusion

To conclude with, the laser beam induced changes to CN-85 polymer track detector have been clearly investigated in this study. The results reveal significant modifications in the optical behavior, photoluminescence property, structure, surface wettability and surface free energy. There is a shift of the UV–Vis spectra toward higher wavelength which leads to a decrease in the band gap energy of irradiated samples. The optical band gap energy decreases from 3.6 to 2.6 eV, for pristine and irradiated sample with the highest dose, respectively. This decrease may be due to the formation of new electronic levels in the forbidden band gap. The increase in carbon atoms per conjugated length confirms the improvement in the irradiated polymer. The PL intensity of pristine sample is larger than that compared to irradiated samples. This reduction in the PL intensity of the irradiated samples is attributed to the presence of impurities and destruction of surface chemical species, which is due to the formation of new radiative recombination levels and also deposition of the energy of the laser beam in the samples. XRD spectra show dominant disorders characters due to cross-linking, which destroy the crystalline structure. The results of the effect of laser beam on the wettability and surface free energy show an enhancement in the polarity of the sample surface, which leads to an increase in the wettability and surface free energy. Thus, the obtained results of CN-85 polymer may be usable for some medical dosimetry and industrial applications such as applications which require the bending without breaking this polymer.

References

Abdul-Kader, A.M., 2009. Photoluminescence and optical properties of He ion bombarded ultra-high molecular weight polyethylene. Appl. Surf. Sci. 255, 5016–5020.

Abdul-Kader, A.M., 2013. The optical band gap and surface free energy of polyethylene modified by electron beam irradiations. J. Nucl. Mater. 435, 231–235.

Abdul-Kader, A.M., El-Badry Basma, A., Zaki, M.F., Hegazy, Tarek M., Hashem, Hany M., 2010. Ion beam modification of surface properties of CR-39. Philos. Mag. 90 (19), 2543–2555.

Abdul-Kader, A.M., El-Gendy, Y.A., Al-Rashdy, Awad A., 2012. Improve the physical and chemical properties of biocompatible polymer material by MeV He ion beam. Radiat. Phys. Chem. 81, 798–802.

Abel, F., Quillet, I.V., Schott, M., 1995. Degradation of polystyrene thin films under d, 4He and 12C irradiation studied by ion beam analysis: effects of energy loss, sample thickness and isotopic content. Nucl. Instrum. Methods Phys. Res. B 105, 86.

Ali, Z.I., Abdul-Kader, A.M., Rizk, R.A., Ali, M., 2013. Tailoring surface properties of polymeric blend material by ion beam bombardment. Radiat. Phys. Chem. 9, 120–124.

Bouffard, S., Balanzat, E., Leroy, C., Busnel, J.P., Guevelou, G., 1997. Cross-links induced by swift heavy ion irradiation in polystyrene. Nucl. Instrum. Methods Phys. Res. B 131, 79.

Calcagno, L., Compagnini, G., Foti, G., 1992. Structural modification of polymer films by ion irradiation. Nucl. Instrum. Methods Phys. Res. B 65, 413.

El-Badry Basma, A., Zaki, M.F., Abdul-Kadder, A.M., Hegazy Tarek, M., Ahmed, Morsy A., 2009. Ion bombardment of poly-allyl-diglycol-carbonate (CR-39). Vacuum 83, 1138.

Gupta, S., Choudhary, D., Sarma, A., 2000. Study of carbonaceous clusters in irradiated polycarbonate with UV–Vis spectroscopy. J. Polym. Sci. Part B: Polym. Phys. 38, 1589–1594.

Hermsdorf, D., 2011. Physics aspects of light particle registration in PADC detectors of type CR-39. Radiat. Meas. 46, 396–404.

Klaumiinzer, S., Zhu, Q.Q., Schnabel, W., 1996. Ion-beam-induced crosslinking of polystyrene – still an unsolved puzzle. Nucl. Instrum. Methods Phys. Res. B 116, 154.

Lounis-Mokrani, Z., Fromm, M., Barillon, R., Chambaudet, A., Allab, M., 2003. Characterization of chemical and optical modifications induced by 22.5 MeV proton beams in CR-39 detectors. Radiat. Meas. 36, 615.

Marletta, G., 1990. Chemical reactions and physical property modifications induced by keV ion beams in polymers. Nucl. Instrum. Methods Phys. Res. B 46, 295.

Owens, D.K., Wendt, R.C., 1969. Estimation of the surface free energy of polymers. J. Appl. Polym. Sci. 13, 1741.

Phukan, T., Kanjilal, D., Goswami, T.D., Das, H.L., 2003. Study of optical properties of swift heavy ion irradiated PADC polymer. Radiat. Meas. 36, 611.

Radwan, M.M., 2001. Structural characterization of diglycol carbonate and polycarbonate SSNTDs irradiated with infrared laser pulses. Radiat. Meas. 33, 183.

Radwan, R.M., 2009. Study of the optical properties of gamma irradiated high-density polyethylene. J. Phys. D Appl. Phys. 42, 015419 (5p).

Ramola, R.C., Chandra, S., Negi, A., Rana, J.M.S., Annapoorni, S., Sonkawade, R.G., Kulriya, P.K., Srivastava, A., 2009. Study of optical band gap, carbonaceous clusters and structuring in CR-39 and PET polymers irradiated by 100 MeV O 7$^+$ ions. Phys. B 404, 26.

Rizk, R.A.M., Abdul-Kader, A.M., Ali, Z.I., Ali, M., 2008. Effect of ion bombardment on the optical properties of LDPE/EPDM polymer blends. Vacuum 83, 805.

Sharma, T., Aggarwal, S., Kumar, S., Mittal, V.K., Kalsi, P.C., Manchanda, V.K., 2007. Effect of gamma irradiation on the optical properties of CR39 polymer. J. Mater. Sci. 42, 1127.

Singh, S., Prasher, S., 2005. The optical, chemical and spectral response of gamma irradiated lexan polymeric track recorder. Radiat. Meas. 40, 50.

Srivastava, A., Singh, T.V., Mule, S., Rajan, C.R., Ponrathnam, S., 2002. Study of chemical, optical and thermal modifications induced by 100 MeV silicon ions in a polycarbonate film. Nucl. Instrum. Methods Phys. Res. B 192, 402.

Steckenreiter, T., Balanzat, E., Fuess, H., Trautmann, C., 1997. Chemical modifications of PET induced by swift heavy ions. Nucl. Instrum. Methods Phys. Res. B 13, 159.

Toth, S., Fule, M., Veres, M., Pocsik, I., Koos, M., Toth, A., Ujvari, T., Bertoti, I., 2006. Photoluminescence of ultra-high molecular weight polyethylene modified by fast atom bombardment. Thin Solid Films 497, 279.

Turos, A., Abdul-Kader, A.M., Grambole, D., Jagielski, J., Piaztkowska, A., Madi, N.K., Al-Maadeed, M., 2006. The effects of ion bombardment of ultra-high molecular weight polyethylene. Nucl. Instrum. Methods B 249, 660.

Urbach, F., 1953. The long-wavelength edge of photographic sensitivity and of the electronic absorption of solids. Phys. Rev. 92, 1324.

Vijay Kumar, Sonkawade, R.G., Chakarvarti, S.K., Kulriya, P., Kant, K., Singh, N.L., Dhaliwal, A.S., 2011. Study of optical, structural and chemical properties of neutron irradiated PADC film. Vacuum 86, 275–279.

Zaki, M.F., 2008. Gamma-induced modification on optical band gap of CR-39 SSNTD. J. Phys. D 41, 175404.

Zaki, M.F., Hegazy, Tarek M., Taha, Doaa H., 2014. Chin. J. Phys. 52 (4). http://dx.doi.org/10.6122/cjp.52.1364.

Zhiyong, Zhu, Yunfan, Jin, Changlong, Liu, Youmei, Sun, Mingdong, Hou, Chonghong, Zhang, Zhiguang, Wang, Jie, Liu, Xiaoxi, Chen, Baoquan, Li, Yanbin, Wang, 2000. Chemical modifications of polystyrene under swift Ar ion irradiation: a study of the energy loss effects. Nucl. Instrum. Methods Phys. Res. B 169, 83.